



HAL
open science

Enhancing properties of lead-free ferroelectric BaTiO₃ through doping

Zechao Li, Jiacheng Yu, Shenglan Hao, Pierre-Eymeric Janolin

► **To cite this version:**

Zechao Li, Jiacheng Yu, Shenglan Hao, Pierre-Eymeric Janolin. Enhancing properties of lead-free ferroelectric BaTiO₃ through doping. *Journal of the European Ceramic Society*, 2022, 42 (12), pp.4693-4701. 10.1016/j.jeurceramsoc.2022.05.023 . hal-03720823

HAL Id: hal-03720823

<https://centralesupelec.hal.science/hal-03720823>

Submitted on 12 Jul 2022

HAL is a multi-disciplinary open access archive for the deposit and dissemination of scientific research documents, whether they are published or not. The documents may come from teaching and research institutions in France or abroad, or from public or private research centers.

L'archive ouverte pluridisciplinaire **HAL**, est destinée au dépôt et à la diffusion de documents scientifiques de niveau recherche, publiés ou non, émanant des établissements d'enseignement et de recherche français ou étrangers, des laboratoires publics ou privés.

Enhancing properties of lead-free ferroelectric BaTiO₃ through doping

Zechao LI, Jiacheng YU, Shenglan HAO, and Pierre-Eymeric JANOLIN*
Université Paris-Saclay, CNRS, CentraleSupélec, laboratoire SPMS, 91190 Gif-sur-Yvette

The substitution on either the *A*- or *B*-site of ferroelectric perovskites by aliovalent elements has a profound influence on their properties. Donor doping “softens” ferroelectrics, whereas acceptor doping “hardens” them. The charge compensation mechanisms are reviewed, as well as the models describing their effects. The focus of this review is doped-BaTiO₃, a model lead-free ferroelectric. The effects of aliovalent doping on its dielectric, ferroelectric, and piezoelectric properties are reviewed and illustrated in the case of Cu (acceptor) doping.

Keywords: *Ceramics, Ferroelectrics, Microstructure, Properties*

I. INTRODUCTION

Ferroelectric materials are characterised by a spontaneous polarisation (\mathbf{P}_s) that can be switched reversibly between at least two different orientations under the application of an electric field.[1–4] Since the first ferroelectric crystals were produced in 1935 by Bush and Scherrer[1], ferroelectric materials have attracted much attention from a wide community due to their numerous properties including dielectric, piezoelectric, pyroelectric, electrocaloric etc. As a consequence, ferroelectric materials are used not only in the fields of information memory, energy storage, and optical devices but also as resonators, transducers, sensors, actuators, and capacitors.[2, 5–8] New ferroelectric materials were gradually discovered and synthesized to satisfy various application needs, such as lead zirconate titanate (PbZr_{1-x}Ti_xO₃), lead lanthanum zirconate titanate (Pb_{1-3y}La_{2y}Zr_{1-x}Ti_xO₃ or Pb_{1-y}La_y(Zr_{1-x}Ti_x)_{1-0.25y}O₃), and barium titanate (BaTiO₃).

BaTiO₃ is a promising candidate for lead-free perovskite oxide (*ABO*₃) ferroelectrics. The Ba²⁺ cation occupies the *A* site at the corners of the perovskite unit cell and each *A*-site cation is 12-fold coordinated with the oxygen anions. At the center of the cell (on the *B* site), the Ti⁴⁺ is surrounded by an oxygen octahedron (6-fold coordination). Doping on either the *A* site [9–11], *B* site [12–14] or both [15, 16] to tune BaTiO₃ properties has been extensively investigated. Indeed, adding suitable dopants to BaTiO₃, even in minute quantity, has a dramatic influence on its electrical properties. For example, M. Acosta *et al.* reviewed the improved piezoelectric properties of doped BaTiO₃,[17] and dielectric properties of rare-earth doped BaTiO₃ were summarized by F. Ismail *et al.*[18] Recently, S. Hao *et al.* investigated the change in optical absorption of co-doped BaTiO₃ ceramics.[19]

Here, we shall review the effects of doping on BaTiO₃ ceramics in terms of dielectric, ferroelectric, and

piezoelectric properties. Moreover, various ferroelectric behaviors of acceptor-doped BaTiO₃ will be systematically illustrated with Cu-doped BaTiO₃.

First, BaTiO₃-based solid solutions should be distinguished from *M*-doped BaTiO₃ based on whether the *M*-based compound can adopt the perovskite structure. If *MTiO*₃ (e.g. SrTiO₃) or Ba*MO*₃ (e.g. BaZrO₃) form a stable perovskite then a solid-solution is usually formed. This is generally the case with isovalent substitution on either the *A* or *B* site of the perovskite and can be predicted based on the Goldschmidt tolerance factor and the octahedral factor.[20] On the contrary, if *MTiO*₃ or Ba*MO*₃ do not form a stable perovskite phase, then there is a maximum amount of *M* that can be introduced in the perovskite structure of BaTiO₃ (usually a few atomic percents). The resulting compounds constitute the *M*-doped BaTiO₃ that are the topic of this review.

Substitutional aliovalent (a.k.a heterovalent) doping is the intentional introduction of dopants with a different valence than the ion for which they substitute in the base material. Common dopants for BaTiO₃ and their valence are shown by green stars (*A*-site doping) and blue circles (*B*-site doping) in Figure.1. Aliovalent dopants can be more or less positively charged than the host ion, therefore defining respectively donors or acceptors.

Doping ferroelectrics with donors (e.g. Rare-Earth ions *RE*³⁺ substituting for Ba²⁺) “softens” them. The “soft” ferroelectrics are characterized by a higher mobility of their domain walls. This is ascribed to the following two mechanisms: the relieved internal stress caused by Ba or Ti vacancies (V''_{Ba} or V''''_{Ti})[22–24] and electrons transfer between ionized Ba and Ti vacancies[23, 25, 26]. The relative importance of each mechanism remains to be determined. In addition, the primary charge compensation mechanism in donor-doped ferroelectrics (Ba vacancies, Ti vacancies, free electrons, changes of valence state of Ti ions...)[9, 10, 27] remains as well an open question[28].

Oppositely, acceptor doping hinders the movement of the domain walls. Ferroelectrics consequently become “hard”[3]. The two main models put forward to explain this are the volume and surface effects.

The volume effect attributes the stabilization of

* Pierre-Eymeric.Janolin@centralesupelec.fr

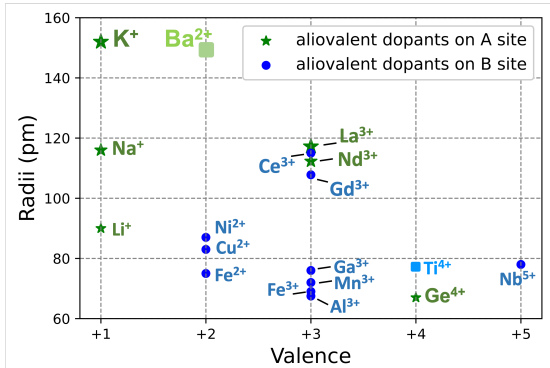


FIG. 1. The radii[21] of common dopants for BaTiO₃. The host ions (Ba²⁺ and Ti⁴⁺) are presented by square symbols and the aliovalent dopants for A site (coordination 12) and B site (coordination 6) of BaTiO₃ are shown by green stars and blue circles respectively.

the domain structure to the oxygen vacancies,[29] accompanying acceptor doping through the formation of defect dipoles ($M-V_{\text{O}}^{\bullet\bullet}$), as shown by EPR measurements on Mn²⁺. [30] These dipoles act as an internal bias field that pins the domains and therefore stiffens the walls.[14, 31, 32] According to the symmetry-conforming principle of point defects, the symmetry of defect dipoles conform to the surrounding crystal symmetry at thermodynamic equilibrium.[33, 34] With oxygen vacancies hopping between neighboring positions next to dopants, defect dipoles achieve reorientation.[35, 36] The surface effect postulates that the oxygen vacancies move to the domain walls or grain boundaries where they fix the domain walls.[31, 37, 38] The aging observed in Mn-doped BaTiO₃ single-domain crystal[39] (devoid of domain walls) or with controlled domain structures[35] strongly supports the volume effect as the main hardening mechanism in ferroelectrics. To illustrate the volume effect at play and the interactions between the defect dipoles and the spontaneous polarisation of the crystal matrix, Cu was chosen as a dopant for its stable vacancy especially in octahedral symmetry. Substituting for Ti, it is therefore an acceptor and will harden BaTiO₃.

II. CHANGING DIELECTRIC PROPERTIES

A. Effect on the permittivity

In ferroelectrics, the domain walls motion is a major contributor to the dielectric properties. The dielectric response is significantly improved by enhancing the 180° domain wall (Figure.2(a)) mobility in tetragonal BaTiO₃ without introducing large dielectric losses, which are mostly caused by 90° domain wall (Figure.2(b)) motion[40] and electronic conduction[10].

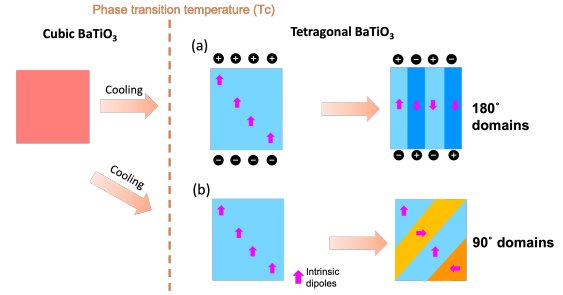


FIG. 2. Schematic of the formation of 180° (a) and 90° (b) domain walls in BaTiO₃. Cooling below the phase transition temperature, the spontaneous polarisation of BaTiO₃ induces surface charges which cause a depolarising field. As a result, 180°-domains with opposite polarisation are created in order to minimize the corresponding electrostatic energy; (b) Simultaneously, 90° domains are created to minimize the mechanical stresses caused by the phase transition.

When BaTiO₃ is doped with donors, A-site vacancies[9, 41], B-site vacancies,[42, 43] and/or electrons[43] are induced for charge balancing. This is the case for example when La³⁺ substitutes for Ba²⁺: $3 \text{Ba}_{\text{Ba}}^{\times} \rightarrow V_{\text{Ba}}^{\prime\prime} + 2 \text{La}_{\text{Ba}}^{\bullet}$ in Ba_{1-3x}La_{2x}TiO₃, $\text{Ba}_{\text{Ba}}^{\times} + \frac{1}{4} \text{Ti}_{\text{Ti}}^{\times} \rightarrow \text{La}_{\text{Ba}}^{\bullet} + \frac{1}{4} V_{\text{Ti}}^{\prime\prime\prime}$ in Ba_{1-y}La_yTi_{1-y/4}O₃, and $\text{Ba}_{\text{Ba}}^{\times} \rightarrow \text{La}_{\text{Ba}}^{\bullet} + e^{-}$ in Ba_{1-z}La_zTiO₃. [9] Due to the softening mechanism of donor doping, the permittivity increases.[3, 44, 45] For example, the relative permittivity reaches 11 800 for A-site Nd³⁺-doped BaTiO₃[41] and 36 000 for A-site La³⁺-Zr⁴⁺ co-doped BaTiO₃[46] compared with 4 500-10 000 in pure BaTiO₃. [47, 48] In addition, the induced electrons from donor doping increase the conduction, resulting in an increase of dielectric losses[10, 11].

In acceptor-doped BaTiO₃, positively charged oxygen vacancies are induced for charge compensation,[36, 39, 49, 50] such as $3 \text{Ti}_{\text{Ti}}^{\times} \rightarrow 2 \text{Ti}_{\text{Ti}}^{\prime\prime} + \text{Ni}_{\text{Ti}}^{\prime\prime} + 2 V_{\text{O}}^{\bullet\bullet}$ in BaTi_{1-x}Ni_xO₃, [16] and $\text{Ba}_{\text{Ba}}^{\times} \rightarrow \text{Li}_{\text{Ba}}^{\prime} + \frac{1}{2} V_{\text{O}}^{\bullet\bullet}$ in Ba_{1-x}Li_{2x}TiO₃. [51]. The existence of oxygen vacancies decreases the mobility of domain walls, contributing to the decrease of the permittivity.[39] For example, with Fe or Mn concentrations increasing to 1 at%, the permittivity of B-site-doped BaTiO₃ decreases to 1 800 or 1 000, respectively; [52] Ce³⁺-Gd³⁺ co-doped BaTiO₃ (on the B site) also exhibits a decreased permittivity as the doping concentration increases.[53] This is also the case for the incorporation (still on the B-site) of Zn²⁺ in BaTiO₃ that decreases the permittivity value by almost 1 000.[54] Even though it is not the case for BaTiO₃ doped with 0.4 at% Cu, permittivity decreases with Cu concentrations increasing to 1.6 at% (Figure.4(a)). Moreover, oxygen vacancies may also contribute to the conductivity, thereby increasing dielectric losses.[55] For example, the

oxygen-deficient $\text{BaTiO}_{3-\delta}$ eventually crosses an insulator-metal transition when δ exceeds 0.25, while retaining its ferroelectric character.[56] In our work, 1.6 at% Cu(acceptor)-doped BaTiO_3 shows higher dielectric loss than undoped sample, as shown in Figure.4(b).

B. Shifting phase transitions

In addition to affecting the permittivity of BaTiO_3 , doping can also change the transition temperatures. At high temperature (above the Curie temperature T_C), BaTiO_3 is paraelectric with a centrosymmetric cubic symmetry ($Pm\bar{3}m$). It undergoes a series of phase transitions to ferroelectric phases: first to a tetragonal ($P4mm$) at $T_C=395\text{K}$, then to an orthorhombic (Amm) phase at $T_{T-O}=280\text{K}$ and finally to a rhombohedral ($R3m$) phase at 185K [1, 3] (see Figure.3).

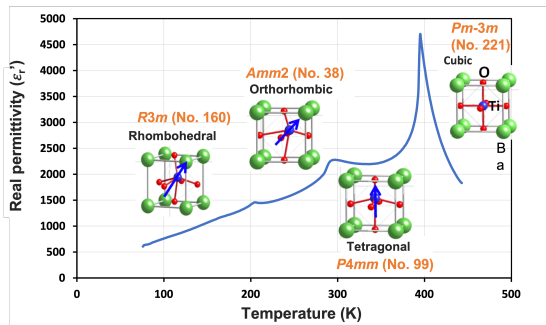


FIG. 3. A real part of the relative permittivity of BaTiO_3 as function of temperature. The insets depict the unit cell, its space group and crystalline systems together with a representation of the polarisation direction.

The phase transitions of BaTiO_3 are mostly displacive and have been interpreted by the displacement of Ti cations relative to O_6 cage. Precisely, the direction of this displacement is determined by the competition between short-range interactions (Pauli repulsion) and long-range interactions (Coulomb attraction, dipole-dipole).[22, 57]

Because dopants have an ionic radius that differs from the one of the host ions, the oxygen octahedron surrounding a dopant is distorted and changes in phase transition temperatures are therefore expected. When smaller ions substitute for Ba^{2+} on the A site ($r_{\text{Ba}^{2+}} = 149\text{pm}$), the surrounding oxygen ions displace towards the dopant, resulting in a more open space enabling the larger displacement of Ti. Such displacement is favored along the $\langle 111 \rangle$ axes rather than along the $\langle 100 \rangle$ axis.[58] As a consequence the tetragonal phase is destabilized and T_C decreases. For example, the T_C of Ce-doped BaTiO_3 ($r_{\text{Ce}^{3+}} = 115\text{pm}$) decreases to 313K for a Ce concentration of 3 at%.[59] The other phase transition tem-

peratures may also be affected. In A -site La-doped BaTiO_3 ($\text{Ba}_{1-x}\text{La}_{2x/3}\text{TiO}_3$ with $r_{\text{La}^{3+}} = 117.2\text{pm}$) T_C decreases while T_{T-O} increases with increasing La concentration until $x=0.06$, resulting in an overall narrower temperature range for the tetragonal phase.[27]

Besides the effects on the A -site, replacing Ti ions ($r_{\text{Ti}^{4+}} = 74.5\text{pm}$) on the B site by dopants with different radii also distorts oxygen octahedra. A destabilization of the tetragonal phase occurs when larger ions substitute for Ti. These larger ions push the adjacent oxygen anions toward the neighboring octahedra, reducing the space for the displacement of Ti ions along $\langle 100 \rangle$ axis. Consequently, the cubic-tetragonal transition (at T_C) is shifted to lower temperatures. The tetragonal-orthogonal phase transition (at T_{O-T}) may also be changed.[58] For example, the T_C and T_{O-T} of $(1-x)\text{BaTiO}_3-x\text{LiF}$ ceramics ($r_{\text{Li}^{+}} = 90\text{pm}$) are decreased to 334K and increased to 298K respectively with increasing x (over the 2-5 at% range).[60] Adding 1 wt% of Zn ($r_{\text{Zn}^{2+}} = 88\text{pm}$) lowers the Curie temperature of BaTiO_3 by 7K .[54] In $\text{BaTi}_{1-x}\text{Mn}_x\text{O}_3$ with 1.3 at% Mn ($r_{\text{Mn}^{2+}} = 97(81)\text{pm}$ and $r_{\text{Mn}^{3+}} = 78.5(72)\text{pm}$ for high (low) spin), the Curie temperature decreases to 383K .[61] In the case of Cu^{2+} ($r_{\text{Cu}^{2+}} = 87\text{pm}$) doping on the B site, as shown in Figure.4, we observed a decrease of both T_C and T_{O-T} for doping levels from 0.4 to 1.6 at%. The lower permittivity of the pure BaTiO_3 sample compared to the 0.4 at% Cu-doped sample is due[62, 63] to the lower grain size of the pure BaTiO_3 sample ($<1\mu\text{m}$, measured by SEM) compared to the 0.4 at% Cu-doped sample (tens of μm). The doping-induced decrease of the permittivity is therefore over-compensated in the doped sample by the larger grain size.

The destabilisation of the tetragonal phase occurs as well when smaller ions substitute on the B -site. Doping with smaller ions such as Al^{3+} ($r_{\text{Al}^{3+}} = 67.5\text{pm}$) on the B site, the octahedra around the dopant shrink and the movement of Ti ions along the $\langle 100 \rangle$ axes is hindered as a consequence. For example, $\text{BaTi}_{0.9992}\text{Al}_{0.0008}\text{O}_3$ has a slightly lower T_C of 390K and an increased T_{O-T} of 324K compared to pure BaTiO_3 .[64]

In summary, the domain walls movement significantly affect the dielectric properties of BaTiO_3 ceramics. Donor doping increases the domain walls mobility and permittivity increases as a consequence. Oppositely, the hardening mechanism of acceptor doping impedes domain rotation, resulting in the decrease of permittivity. In addition, oxygen vacancies induced by acceptor doping and electrons induced by donor doping both contribute to conduction. Dielectric losses increase as a consequence. Due to the different ionic radii between dopants and host ions, distortion of oxygen octahedra in the lattice are induced and displacements of Ti ions along $\langle 100 \rangle$ axis

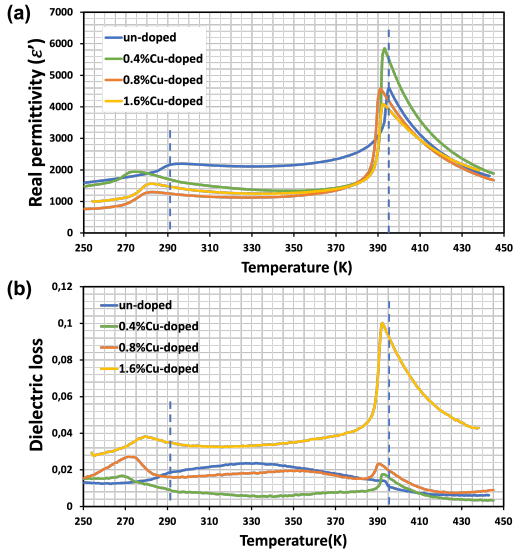


FIG. 4. Doping effect on the real part of the relative permittivity (a) and dielectric losses (b) of Cu-doped BaTiO₃ with different doping concentration (at 10 kHz) as function of temperature, compared to the un-doped BaTiO₃.

are reduced. Consequently, the Curie temperatures of doped-BaTiO₃ are shifted to lower temperatures and the tetragonal phase is destabilized.

III. CHANGING FERROELECTRIC PROPERTIES

A. Softening or hardening ceramics

The hysteresis loop (P-E loop) is the defining characteristic of ferroelectric materials. It presents the polarisation response to an external electric field. Figure.5 shows the hysteresis loop of pure BaTiO₃ ceramics with schematics of the corresponding domains arrangements.

After sintering, BaTiO₃ ceramics exhibit a zero net polarisation, due to the random orientation of the ferroelectric domains. Upon increasing external electric field, domains gradually align through domain walls movement. The polarisation gradually increases and then saturates (up to P_s) under high fields. Upon removal of the external field, not all domains switch back to their original orientation, resulting in a remanent polarisation (P_r) in the ceramic. The area decorated by diagonal stripes in Figure.5 represents the recoverable energy (W_{reco}). It corresponds to the total electric energy brought to the system minus the part used in the polarisation process of the ceramic, represented by the solid blue area inside the hysteresis loop.

Ferroelectrics have higher saturation polarisations and breakdown strengths than other bulk dielec-

tric ceramics,[7, 65] which are beneficial to the total stored energy (W_{total} , solid blue area in Figure.5). However, their W_{reco} is lower due to the high value of the remanent polarisation. Doping can be used to decrease the remanent polarisation while keeping a high saturation polarisation, thereby decreasing the hysteresis losses (or increasing W_{reco}) while keeping a high W_{total} . [66]

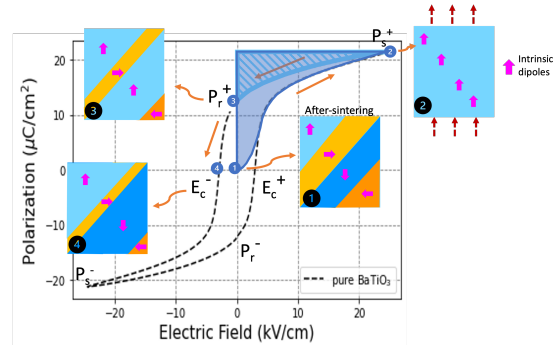


FIG. 5. Hysteresis loop of pure BaTiO₃ at room temperature with corresponding dipoles orientation (inserts). The initially randomly-oriented dipoles are gradually aligned by the increasing external electric field. BaTiO₃ goes from state 1 (“virgin” state) to state 2 (polarised state). Under removal of the field, dipoles partially switch back (state 3 with remanent polarisation P_r^+). At the coercive field (E_c^-) the orientations of the dipoles cancel each other. The total stored energy (W_{total}) is presented by solid blue area and the diagonal-stripe area corresponds to the recoverable energy (W_{reco}).

Donor-doping presents the advantages of “soft” materials: higher domain-wall mobility, slimmer hysteresis loops, lower coercive fields, all contributing to the decrease of energy losses and therefore to the increase of W_{reco} . [67–69] Through the volume effect, acceptor doping not only “hardens” ferroelectrics with decreased domain-wall mobility but can also result in pinched hysteresis loops. The resulting lower remanent polarisation, higher coercive field, and lower saturation polarisation [70, 71] of such double loops compared to the open loop of pure BaTiO₃ are illustrated in Figure.6 for Cu-doped BaTiO₃. Significantly, the much smaller remanent polarisation increases W_{reco} despite a small decrease of the saturation polarisation. [66, 72] At thermodynamic equilibrium, the defect dipoles created by acceptor doping are aligned with the crystal symmetry (insert for state 1 in Figure.6), a feature described by the symmetry-conforming principle. [33] The orientation of the defect dipoles is not modified by the application of the electric field [30, 45] as it would necessitate the diffusion of the oxygen vacancies from one site to another. [12] The random distribution of defect dipoles produces a restoring force that accelerates the domain back-switching to their original state (state 1) in which the ceramics have a zero net

polarisation.[7, 22] The resulting pinching of the hysteresis loop enhances W_{reco} .

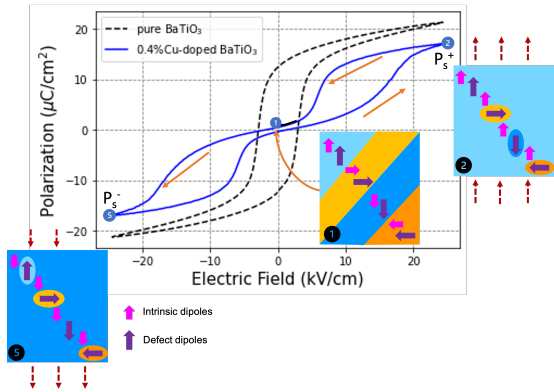


FIG. 6. Hysteresis loop pinching process for 0.4 at% Cu-doped BaTiO_3 (solid blue line) compared to the open loop of pure BaTiO_3 (dotted black line) at room temperature. The positive electric field gradually aligns the intrinsic dipoles and moves the domain walls except around the defect dipoles, as shown from state 1 to state 2. When the external field is removed, the defect dipoles produce a restoring force that switches intrinsic dipoles back to their initially random orientations and ceramics have a near zero net polarisation. The same behaviour happens under the negative electric field (between state 1 and state 5).

Hence, both the slimmer hysteresis loops caused by donor doping or the pinched hysteresis loops induced by acceptor doping are promising methods to increase the recoverable stored energy in doped-ferroelectric ceramics.[66, 72]

B. De-aging and re-aging

The hysteresis loop pinching process is also called aging, which is different from degradation. Degradation is an irreversible exhaustion-type process characterised by decreasing spontaneous and saturation polarisations values.[73] On the contrary, ageing is a reversible process.[66, 74, 75]

The reverse process, de-aging, corresponds to the re-opening of a pinched hysteresis loop. A de-aged sample exhibits a classical ferroelectric P-E loop. This transformation from pinched to open loop (de-aging) is also referred to as from “clamped” to “free” [76] or “unclamped” [77]. As oxygen vacancies migrate and disorder, the defect dipoles temporarily disappear [78–80]. Domains are therefore released, resulting in the de-aging process. Two methods can be used to de-age an aged sample (*i.e.* to open pinched loops): quenching and fatigue treatment.

Quenching consists in heating the sample in its paraelectric phase (over the Curie temperature), where intrinsic dipoles do not exist and oxygen vacancies are disordered (*i.e.* are not necessarily nearest-

neighbors to dopants) before quickly cooling the sample to room temperature. After quenching, defect dipoles are not immediately created as the oxygen vacancies need time to diffuse to positions nearest-neighbor to dopants. The ferroelectric domains are therefore not pinned by the defect dipoles and the hysteresis loop is akin to the one of an un-doped sample. Figure.7(a) illustrates this for Cu-doped BaTiO_3 ceramics quenched in water: the sample initially exhibits a zero polarisation (consistent with a “virgin” state where the intrinsic dipoles are randomly oriented) before an open and symmetric hysteresis loop is measured. The result of this quenching procedure depends however on the thermal conductivity of the cooling environment: for example partially pinched loops were observed in $\text{Pb}(\text{Zr}_{0.58}\text{Ti}_{0.42})\text{O}_3$ cooled in air whereas totally open loops were observed when cooled in water.[3]

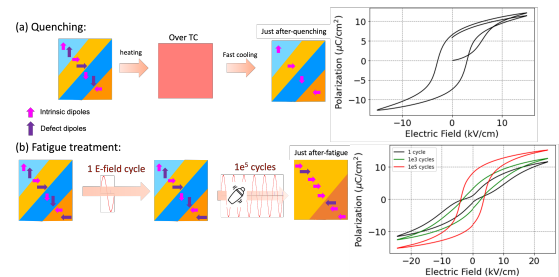


FIG. 7. De-aging processes of a 0.4 at% Cu-doped BaTiO_3 ceramic: (a) Only intrinsic dipoles exist after quenching and the hysteresis loop is open, starting from a “virgin” state with zero net polarisation, (b) Fatigue treatment randomizes the dipoles in the direction of external fields and defect dipoles are almost eliminated due to disordered oxygen vacancies; the pinched hysteresis loop (black curve) gradually opens (green curve) before reaching a stable open shape after 10^5 cycles (red curve).

The other procedure to open a pinched loop is the fatigue treatment where an oscillating electric field is applied numerous times on the sample. As a result, oxygen vacancies disorder, causing the defect dipoles to disappear. As shown in Figure.7(b), the remanent polarisation of 0.4 at% Cu-doped BaTiO_3 increases from the first to the 10^3 cycles (from black curve to green curve) and the hysteresis loop is fully open after 10^5 cycles (red curve). The fatigue characteristics depend on the nature of the ferroelectric material itself, the type of dopants and their concentration, the temperature, and the field profile, among other parameters.[81–85]

If a pinched loop can be opened, the inverse is also possible: it is called re-aging. As shown in Figure.8 a 0.4 at% Cu-doped BaTiO_3 sample exhibits a pinched hysteresis loop once thermodynamic equilibrium is reached, *i.e.* when oxygen vacancies have had enough time to reach positions that are nearest neighbor to dopants, forming defect dipoles. The re-aging pro-

cess not only involves the nucleation and growth of domains[75], but is also driven by the reorientation of defect dipoles. Hence, the ability to re-age doped ferroelectrics depends on the type of dopants, their concentration, and thermal activation.[86, 87]

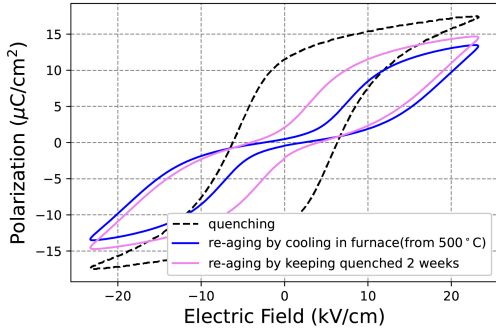


FIG. 8. Re-pinned hysteresis loops of 0.4 at%Cu-doped BaTiO₃. The open loop (“quenching”, dotted black curve) is measured immediately after quenching the sample from above T_C and results from the disordering of the oxygen vacancies. Keeping this quenched sample for two weeks at room temperature, the disordered oxygen vacancies diffuse to positions nearest-neighbor to dopants, which forms defect dipoles and pinches the hysteresis loop (violet curve). Cooling the sample from 500°C (over T_C) in air also gives enough time for the diffusion of oxygen vacancies and the formation of defect dipoles, pinching the hysteresis loop (blue curve) as a consequence.

C. Shifting hysteresis loop

Hysteresis loops of doped ferroelectrics are sometimes shifted along the field axis, as shown in Figure.9(a) where the negative coercive field is larger than the positive one ($\|E_c^-\| > \|E_c^+\|$). This phenomenon is related to the preferential orientation of the defect dipoles that pin the surrounding intrinsic dipoles alongside them. The preferential orientation of defects dipoles acts as an effective internal bias field.[31, 88] As a consequence, a larger opposite external field is needed to switch the polarisation, thereby increasing the corresponding coercive field and shifting the whole hysteresis loop horizontally (Figure.9(a)).[3, 88] Such a shift can be induced through a field-cooling procedure (polarizing ceramic from high temperature (over T_C) to room temperature) in order to align the intrinsic domains. According to the symmetry-conforming defect principle, once equilibrium is reached, the defect dipoles are aligned as well. This is illustrated by the schematics in Figure.9.

The effect of field cooling is evidenced by the non-zero initial polarisation, almost equal to the remanent polarisation. As the defect dipoles eventually

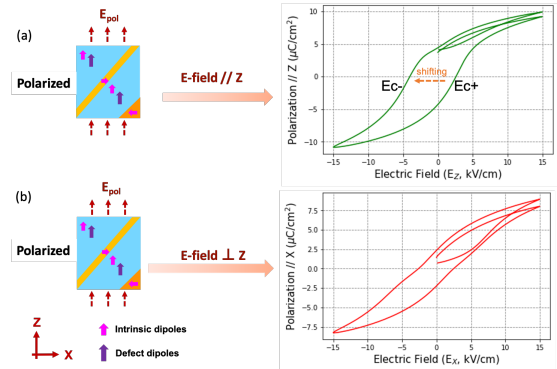


FIG. 9. Hysteresis loops of field-cooled 0.4 at%Cu-doped BaTiO₃ measured (a) along the direction of the poling field (E_{pol}) and (b) along an orthogonal direction. Preferentially-oriented defect dipoles (a) shift the hysteresis loop along the poling field axis and (b) cause a slight pinching of the hysteresis loop measured with a measuring field along an orthogonal direction.

point along the direction the field was applied during field-cooling, they do not provide a perpendicular restoring force. As a consequence, the polarisation loop measured along that direction is not pinched. However, in the direction perpendicular to the poling field direction (Figure.9(b)), the initial polarisation is almost zero. This is because few intrinsic dipoles point perpendicularly to the direction of the poling field. And for those who do, they have a random orientation in that plane. What is more, the few defect dipoles present in that plane adopt a random orientation through the symmetry conforming principle, resulting in the slight pinching of the hysteresis loop measured in that plane. A reduced saturation polarisation is also measured as the majority of defect dipoles still point along the poling direction and therefore hinder the rotation of their surrounding (intrinsic) domains to follow the applied field.

Several days after the field-cooling procedure, the shifted hysteresis loop gets further distorted. An hummingbird-like loop eventually appears, as shown in Figure.10. This is ascribed to the increasing amount of polarised defect dipoles (reaching an equilibrium configuration) leading to stronger pinning effect of the surrounding domains. Such loop is characterised by an asymmetry with the “beak” indicating the majority orientation of the defect dipoles. Under positive electric field (i.e. along defect dipoles majority orientation) domains rotation is facilitated, resulting in a smaller value of the coercive field and reduced hysteresis losses. Under reverse electric field, domain reversal is sluggish with larger hysteresis losses and requires a higher coercive field value.

In summary, the shape of the hysteresis loop can be manipulated through the control of defect dipoles. A pinched loop is induced when the oxygen vacancies are nearest-neighbors to aliovalent dopants, thereby

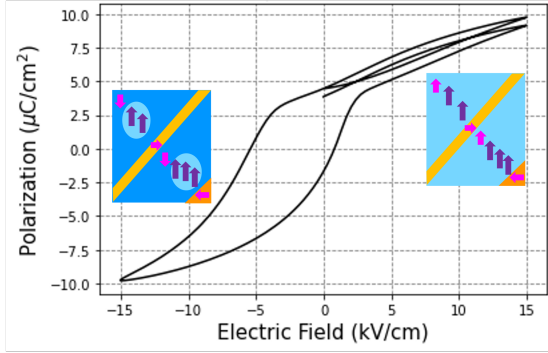


FIG. 10. Humming-bird-like hysteresis loop for 0.4 at% Cu-doped BaTiO₃ caused by the preferential orientation of defect dipoles. Under positive electric field (majority orientation of defect dipoles), domains rotation is easy (small E_c) with low hysteresis loss. Under reverse electric field, domain reversal is sluggish with larger hysteresis losses and higher coercive field.

creating defect dipoles. These defect dipoles provide a restoring force pinching the hysteresis or even inducing a double hysteresis loop akin to the ones of antiferroelectrics. The sample nevertheless remains ferroelectric as the low field state is similar to the “virgin state” of undoped samples after synthesis. Such pinched hysteresis is beneficial, *e.g.* for energy-storage properties.[66, 72]

A classical, open, ferroelectric hysteresis loop can nevertheless be induced in such samples by disordering the oxygen vacancies. This can be achieved immediately after having quenched the sample from its paraelectric phase to room temperature or through fatigue measurements. The induced states (akin to classical ferroelectrics) are nevertheless only metastable and will lead, at thermodynamic equilibrium, to a pinched loop once the oxygen vacancies have had the time to reach positions nearest-neighbor to dopants and form defect dipoles.

In addition to a shape change of the hysteresis loops, doping can also shift the hysteresis loops along the field axis. This shift is due to the internal bias field induced by a preferential orientation of the defect dipoles. Such effect is exacerbated when the sample is poled through field cooling, thereby aligning the majority of the intrinsic dipoles. When thermodynamic equilibrium is reached, most defect dipoles align with the polarised ferroelectric domains and a hummingbird-like hysteresis is generated, with the “beak” along the direction of the majority defect dipoles.

IV. CHANGING ELECTROMECHANICAL PROPERTIES

Doping can also influence the piezoelectric properties of BaTiO₃. The contributions to strain-electric

field relationship are a very complex problem. Apart from the intrinsic lattice strain, domain walls movement account for as much as 50% of the electromechanical effect on ferroelectric materials.[89, 90] In addition, large nonlinear and recoverable electrostrains are most often experimentally observed due to the existence of non-180° domain walls.[1, 22, 91, 92] Thus, the factors affecting the domain walls motions have a major influence over the electromechanical response of BaTiO₃. These factors include the symmetry of the crystal structure, dopants, defects, local variations in the composition, and external excitations such as temperature and electric field.[93, 94]

Compared to the pinned domain walls in “hard” ferroelectric, “soft” ferroelectrics have more mobile domain walls that result in higher electric-field-induced strain.[23, 25, 93, 95] As shown in Table I, the “soft” lead zirconate titanate (PZT-5A, PZT-5H) ceramics have larger piezoelectric coefficients than the “hard” PZT (unaged).[96] Unaged “hard” Ce-doped BaTiO₃ exhibits a lower piezoelectric coefficient than pure BaTiO₃ ($d_{33} = 190 \text{ pm V}^{-1}$).[17, 28]

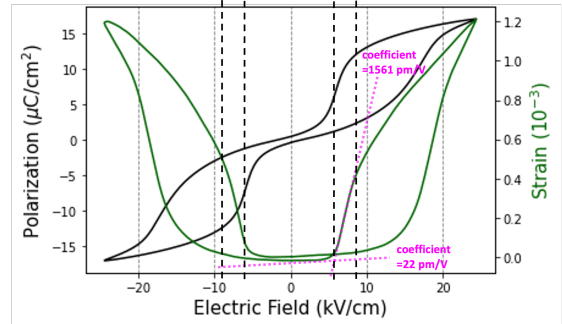


FIG. 11. The polarisation hysteresis loop and strain vs electric field curve of 0.4 at% Cu-doped BaTiO₃. In the lower field range (0-5 kV cm⁻¹ or -5-0 kV cm⁻¹), the strain curve is almost flat with a corresponding piezoelectric coefficient of 22 pm V⁻¹. With decreasing electric field from 8(-8) to 5(-5) kV cm⁻¹, strain drastically and linearly decreases with a piezoelectric coefficient of about 1561 pm V⁻¹.

As shown before, the defect dipoles in the aged state provide a restoring force that eases the domain rotation back to the zero net polarization (virgin) state, pinching the hysteresis loop. Consequently, the apparent piezoelectric coefficient (d_{33}) is drastically increased.[13, 17, 88] As shown in Figure.11, the slope of the strain response of 0.4 at% Cu-doped BaTiO₃ corresponds to a very large piezoelectric coefficient (d_{33}) of 1561 pm V⁻¹ for electric fields in the range of 5 to 8 kV cm⁻¹. Similarly, a d_{33} of 2100 pm V⁻¹ for electric fields from 2.5 to 3.5 kV cm⁻¹ has been reported for aged BaTiO₃ doped with 0.3 at%Mn. Single crystals of aged 0.02 at%Fe-doped BaTiO₃ also present large strain (7.5×10^{-3}) at low electric field (2 kV cm⁻¹), corresponding to a d_{33} of 3750 pm V⁻¹[88] about 10 times

TABLE I. Comparison of piezoelectric coefficient (d_{33}) values between soft and hard ferroelectrics (PZT: lead zirconate titanate and BT: barium titanate) at room temperature.

Composition	Soft PZT		Hard PZT (unaged)			Hard BT (unaged)	Hard BT (aged)	
	PZT-5A	PZT-5H	PZT-2	PZT-4	PZT-8	2 at%Ce	0.3 at%Mn	0.02 at%Fe
d_{33} (pm V ⁻¹)	375	590	152	290	225	116	2100	3750
Reference	[96]	[96]	[93]	[96]	[96]	[28]	[14]	[88]

larger than conventional piezoelectric PZT (see Table I) and $\text{Pb}(\text{Zn}_{1/3}, \text{Nb}_{2/3})\text{O}_3$ -8% PbTiO_3 (PZN-PT) ceramics[97].

In summary, the enhanced mobility of domain walls enhances the piezoelectric properties of “soft” ferroelectrics compared to their un-doped counterparts. In aged hard ferroelectrics the restoring force induced by the defect dipoles accelerates the domain rotation back to their initial orientation. As a result, the piezoelectric coefficients of aged BaTiO_3 are significantly increased, reaching values over 1500 pm V⁻¹ (this work and Refs.[14, 88]). This defect dipoles-domains interaction created by acceptor doping provides a promising method to realize applications based on enhanced electromechanical properties of BaTiO_3 .

V. CONCLUSION

Doping provides a promising opportunity to tune the dielectric, ferroelectric, and piezoelectric properties of environmentally-friendly BaTiO_3 ceramics.

Because of the different ionic radii between dopants and host ions, the oxygen octahedra of the perovskite structure distort and the displacement of Ti ions along the $\langle 100 \rangle$ axis is affected, which results in the destabilization of the tetragonal phase and a decrease of the Curie temperature compared to pure BaTiO_3 .

Donor doping improves the mobility of domain walls and BaTiO_3 is consequently “softened”. The “softening” mechanism is ascribed to the reduced internal stress caused by Ba or Ti vacancies and to electron transfer between Ba and Ti vacancies.[22–26] Macroscopically, permittivity is increased and slimmer hysteresis loops with lower coercive fields are measured, increasing the energy storage performance. Another advantage of “soft” materials is their higher piezoelectricity compared to un-doped counterparts.

For acceptor-doped BaTiO_3 , the volume effect (defect-dipoles created by oxygen vacancies nearest-neighbors to dopants) as the primary hardening mechanism decreases mobility of domain walls, which has a contribution to decrease permittivity. According to the symmetry-conforming principle, the defect dipoles formed by oxygen vacancies accompanying acceptor dopants are aligned by crystal symmetry at thermodynamic equilibrium. Hence, aging process results in double hysteresis loops thereby increasing the recoverable energy storage. Through the control of the defect dipoles orientation, the shape of the hysteresis loop can be manipulated including pinching, opening, re-pinching, shifting, even distorting to a hummingbird-like hysteresis loop. Moreover, aged doped- BaTiO_3 shows higher piezoelectric coefficients due to the restoring force of the defect dipoles.

References

- [1] Malcolm E Lines and Alastair M Glass. *Principles and applications of ferroelectrics and related materials*. Oxford university press, 2001.
- [2] SM Said, MFM Sabri, and F Salleh. *Ferroelectrics and their applications*. 2017.
- [3] Dragan Damjanovic. Hysteresis in piezoelectric and ferroelectric materials. *The science of hysteresis*, 3:337–465, 2006.
- [4] Irinela Chilibon and José N Marat-Mendes. Ferroelectric ceramics by sol-gel methods and applications: a review. *Journal of sol-gel science and technology*, 64(3):571–611, 2012.
- [5] JF Scott. Applications of modern ferroelectrics. *science*, 315(5814):954–959, 2007.
- [6] Letao Yang, Xi Kong, Fei Li, Hua Hao, Zhenxiang Cheng, Hanxing Liu, Jing-Feng Li, and Shujun Zhang. Perovskite lead-free dielectrics for energy storage applications. *Progress in Materials Science*, 102:72–108, 2019.
- [7] Xihong Hao. A review on the dielectric materials for high energy-storage application. *Journal of Advanced Dielectrics*, 3(01):1330001, 2013.
- [8] Nava Setter and EL Colla. *Ferroelectric ceramics: tutorial reviews, theory, processing, and applications*. Springer, 1993.
- [9] Jia Liu, Lajun Liu, Jiale Zhang, Li Jin, Dawei Wang, Jie Wei, Zuo-Guang Ye, and Chun-Lin Jia. Charge effects in donor-doped perovskite ferroelectrics. *Journal of the American Ceramic Society*, 103(9):5392–5399, 2020.

- [10] Colin L Freeman, James A Dawson, Hung-Ru Chen, Liubin Ben, John H Harding, Finlay D Morrison, Derek C Sinclair, and Anthony R West. Energetics of donor-doping, metal vacancies, and oxygen-loss in a-site rare-earth-doped batio3. *Advanced Functional Materials*, 23(31):3925–3928, 2013.
- [11] T Sareein, P Baipaywad, W Chaiammad, A Ngamjarurojana, S Ananta, X Tan, and R Yimmirun. Dielectric aging behavior in a-site hybrid-doped batio3 ceramics. *Current Applied Physics*, 11(3):S90–S94, 2011.
- [12] Yuji Noguchi, Hiroki Matsuo, Yuuki Kitanaka, and Masaru Miyayama. Ferroelectrics with a controlled oxygen-vacancy distribution by design. *Scientific reports*, 9(1):1–10, 2019.
- [13] Wenfeng Liu, Wei Chen, Liu Yang, Lixue Zhang, Yu Wang, Chao Zhou, Shengtao Li, and Xiaobing Ren. Ferroelectric aging effect in hybrid-doped ba ti o 3 ceramics and the associated large recoverable electrostrain. *Applied physics letters*, 89(17):172908, 2006.
- [14] LX Zhang and X Ren. In situ observation of reversible domain switching in aged mn-doped batio 3 single crystals. *Physical Review B*, 71(17):174108, 2005.
- [15] Da-Yong Lu, Xiu-Yun Sun, and Masayuki Toda. A novel high-k 'y5v'barium titanate ceramics co-doped with lanthanum and cerium. *Journal of Physics and Chemistry of Solids*, 68(4):650–664, 2007.
- [16] Chenjie Fu, Nan Chen, and Guoping Du. Comparative studies of nickel doping effects at a and b sites of batio3 ceramics on their crystal structures and dielectric and ferroelectric properties. *Ceramics International*, 43(17):15927–15931, 2017.
- [17] Matias Acosta, N Novak, V Rojas, S Patel, R Vaish, J Koruza, GA Rossetti Jr, and J Rödel. Batio3-based piezoelectrics: Fundamentals, current status, and perspectives. *Applied Physics Reviews*, 4(4):041305, 2017.
- [18] Fatin Adila Ismail, Rozana Aina Maulat Osman, and Mohd Sobri Idris. Review on dielectric properties of rare earth doped barium titanate. In *AIP Conference Proceedings*, volume 1756, page 090005. AIP Publishing LLC, 2016.
- [19] Shenglan Hao, Minghai Yao, Gaëlle Vitali Derrien, Pascale Gemeiner, Mojca Otoničar, Pascal Ruello, Houssny Bouyanff, Pierre-Eymeric Janolin, Brahim Dkhil, and Charles Paillard. Optical absorption by design in a ferroelectric: co-doping in batio3. *Journal of Materials Chemistry C*, 2021.
- [20] Chonghea Li, Xionggang Lu, Weizhong Ding, Liming Feng, Yonghui Gao, and Ziming Guo. Formability of abx3 (x= f, cl, br, i) halide perovskites. *Acta Crystallographica Section B: Structural Science*, 64(6):702–707, 2008.
- [21] Robert D Shannon. Revised effective ionic radii and systematic studies of interatomic distances in halides and chalcogenides. *Acta crystallographica section A: crystal physics, diffraction, theoretical and general crystallography*, 32(5):751–767, 1976.
- [22] Dragan Damjanovic. Ferroelectric, dielectric and piezoelectric properties of ferroelectric thin films and ceramics. *Reports on Progress in Physics*, 61(9):1267, 1998.
- [23] MI Morozov and D Damjanovic. Charge migration in pb (zr, ti) o 3 ceramics and its relation to ageing, hardening, and softening. *Journal of Applied Physics*, 107(3):034106, 2010.
- [24] Robert Gerson. Variation in ferroelectric characteristics of lead zirconate titanate ceramics due to minor chemical modifications. *Journal of Applied Physics*, 31(1):188–194, 1960.
- [25] Lucien Eyraud, Benoit Guiffard, Laurent Lebrun, and Daniel Guyomar. Interpretation of the softening effect in pzt ceramics near the morphotropic phase boundary. *Ferroelectrics*, 330(1):51–60, 2006.
- [26] J Daniels et al. Electrical conductivity at high temperatures of donor-doped barium titanate ceramics. i. 1976.
- [27] M Ganguly, SK Rout, TP Sinha, SK Sharma, HY Park, CW Ahn, and IW Kim. Characterization and rietveld refinement of a-site deficient lanthanum doped barium titanate. *Journal of alloys and compounds*, 579:473–484, 2013.
- [28] Chen Ang, Zhi Yu, Zhi Jing, Ruyan Guo, AS Bhalla, and LE Cross. Piezoelectric and electrostrictive strain behavior of ce-doped batio 3 ceramics. *Applied physics letters*, 80(18):3424–3426, 2002.
- [29] DM Smyth. Barium titanate. *The Defect Chemistry of Metal Oxides*, pages 253–282, 2000.
- [30] Lixue Zhang, Emre Erdem, Xiaobing Ren, and Rüdiger-A Eichel. Reorientation of (mn ti - vo●●)× defect dipoles in acceptor-modified batio 3 single crystals: An electron paramagnetic resonance study. *Applied Physics Letters*, 93(20):202901, 2008.
- [31] KHHK Carl and KH Hardtl. Electrical after-effects in pb (ti, zr) o3 ceramics. *Ferroelectrics*, 17(1):473–486, 1977.
- [32] G Arlt and H Neumann. Internal bias in ferroelectric ceramics: origin and time dependence. *Ferroelectrics*, 87(1):109–120, 1988.
- [33] Xiaobing Ren. Giant electric-field induced strain in ferroelectric crystals by point-defect mediated reversible domain switching. In *APS March Meeting Abstracts*, volume 2004, pages W19–005, 2004.
- [34] Xiaobing Ren and Kazuhiro Otsuka. Universal symmetry property of point defects in crystals. *Physical review letters*, 85(5):1016, 2000.
- [35] PV Lambeck and GH Jonker. The nature of domain stabilization in ferroelectric perovskites. *Journal of Physics and Chemistry of Solids*, 47(5):453–461, 1986.
- [36] Rüdiger-A Eichel. Defect structure of oxide ferroelectrics—valence state, site of incorporation, mechanisms of charge compensation and internal bias fields. *Journal of electroceramics*, 19(1):11–23, 2007.
- [37] Yuri A Genenko, Julia Glaum, Michael J Hoffmann, and Karsten Albe. Mechanisms of aging and fatigue in ferroelectrics. *Materials Science and Engineering: B*, 192:52–82, 2015.
- [38] HL Stadler. Etched hillocks in batio3. *Journal of Applied Physics*, 34(3):570–573, 1963.
- [39] Lixue Zhang and Xiaobing Ren. Aging behavior in single-domain mn-doped batio 3 crystals: implication for a unified microscopic explanation of ferroelectric aging. *Physical Review B*,

- 73(9):094121, 2006.
- [40] QM Zhang, Haimin Wang, N Kim, and LE Cross. Direct evaluation of domain-wall and intrinsic contributions to the dielectric and piezoelectric response and their temperature dependence on lead zirconate-titanate ceramics. *Journal of Applied Physics*, 75(1):454–459, 1994.
- [41] Zhonghua Yao, Hanxing Liu, Yan Liu, Zhaohui Wu, Zongyang Shen, Yang Liu, and Minghe Cao. Structure and dielectric behavior of nd-doped batio3 perovskites. *Materials Chemistry and Physics*, 109(2-3):475–481, 2008.
- [42] Janusz Nowotny and Mieczyslaw Rekas. Defect structure, electrical properties and transport in barium titanate. vii. chemical diffusion in nb-doped batio3. *Ceramics International*, 20(4):265–275, 1994.
- [43] Helen M Chan, MARTIN R HARMER, and DONALD ML SMYTH. Compensating defects in highly donor-doped batio3. *Journal of the American Ceramic Society*, 69(6):507–510, 1986.
- [44] Qiaomei Sun, Qilin Gu, Kongjun Zhu, Rongying Jin, Jinsong Liu, Jing Wang, and Jinhao Qiu. Crystalline structure, defect chemistry and room temperature colossal permittivity of nd-doped barium titanate. *Scientific reports*, 7:42274, 2017.
- [45] Jiandang Liu, L Jin, Z Jiang, Laijun Liu, L Himanen, J Wei, Nan Zhang, Dawei Wang, and C-L Jia. Understanding doped perovskite ferroelectrics with defective dipole model. *The Journal of chemical physics*, 149(24):244122, 2018.
- [46] Anthony R West, Timothy B Adams, Finlay D Morrison, and Derek C Sinclair. Novel high capacitance materials:-batio3: La and cacu3ti4o12. *Journal of the European Ceramic Society*, 24(6):1439–1448, 2004.
- [47] Vincenzo Buscaglia, Maria Teresa Buscaglia, and Giovanna Canu. Batio3-based ceramics: Fundamentals, properties and applications. 2020.
- [48] Jung-Kun Lee, Kug-Sun Hong, and Jin-Wook Jang. Roles of ba/ti ratios in the dielectric properties of batio3 ceramics. *Journal of the American Ceramic Society*, 84(9):2001–2006, 2001.
- [49] NV Dang, TD Thanh, LV Hong, VD Lam, and The-Long Phan. Structural, optical and magnetic properties of polycrystalline batil- xfexo3 ceramics. *Journal of Applied Physics*, 110(4):043914, 2011.
- [50] Tao Li, Kun Yang, Renzhong Xue, Yuncai Xue, and Zhenping Chen. The effect of cuo doping on the microstructures and dielectric properties of batio 3 ceramics. *Journal of Materials Science: Materials in Electronics*, 22(7):838–842, 2011.
- [51] C Meric Guvenc and Umut Adem. Influence of aging on electrocaloric effect in li+ doped batio3 ceramics. *Journal of Alloys and Compounds*, 791:674–680, 2019.
- [52] H-J Hagemann. Loss mechanisms and domain stabilisation in doped batio3. *Journal of Physics C: Solid State Physics*, 11(15):3333, 1978.
- [53] Kang Yan, Fangfang Wang, Dawei Wu, Xiaobing Ren, and Kongjun Zhu. Ferroelectric aging effects and large recoverable electrostrain in ceria-doped batio3 ceramics. *Journal of the American Ceramic Society*, 102(5):2611–2618, 2019.
- [54] AC Caballero, JF Fernandez, C Moure, and P Duran. Zno-doped batio3: microstructure and electrical properties. *Journal of the European ceramic society*, 17(4):513–523, 1997.
- [55] A Salhi, S Sayouri, A Alimoussa, and L Kadira. Impedance spectroscopy analysis of ca doped batio3 ferroelectric ceramic manufactured with a new synthesis technique. *Materials Today: Proceedings*, 13:1248–1258, 2019.
- [56] I-K Jeong, Seunghun Lee, Se-Young Jeong, CJ Won, N Hur, and A Llobet. Structural evolution across the insulator-metal transition in oxygen-deficient batio 3- δ studied using neutron total scattering and rietveld analysis. *Physical Review B*, 84(6):064125, 2011.
- [57] Shuangyi Liu, Limin Huang, Jackie Li, and Stephen O'Brien. Intrinsic dielectric frequency dependent spectrum of a single domain tetragonal batio3. *Journal of Applied Physics*, 112(1):014108, 2012.
- [58] JN Lin and TB Wu. Effects of isovalent substitutions on lattice softening and transition character of batio3 solid solutions. *Journal of applied physics*, 68(3):985–993, 1990.
- [59] Sabina Yasmm, Shamima Choudhury, MA Hakim, AH Bhuiyan, and MJ Rahman. Effect of cerium doping on microstructure and dielectric properties of batio3 ceramics. *Journal of Materials Science & Technology*, 27(8):759–763, 2011.
- [60] Wei-Gang Yang, Bo-Ping Zhang, Nan Ma, and Lei Zhao. High piezoelectric properties of batio3-xlif ceramics sintered at low temperatures. *Journal of the European Ceramic Society*, 32(4):899–904, 2012.
- [61] Wei Chen, Xia Zhao, Jingen Sun, Lixue Zhang, and Lisheng Zhong. Effect of the mn doping concentration on the dielectric and ferroelectric properties of different-routes-fabricated batio3-based ceramics. *Journal of Alloys and Compounds*, 670:48–54, 2016.
- [62] Jan Petzelt. Dielectric grain-size effect in high-permittivity ceramics. *Ferroelectrics*, 400(1):117–134, 2010.
- [63] Y. Tan, J. Zhang, Y. Wu, C Wang, V Koval, B Shi, H Ye, R McKinnon, G. Viola, and H Yan. *Scientific Reports*, 5:9953, 2015.
- [64] K Vani and Viswanathan Kumar. Evolution of dielectric and ferroelectric relaxor states in al3+-doped batio3. *AIP Advances*, 5(2):027135, 2015.
- [65] Mahesh Peddigari, Haribabu Palneedi, Geon-Tae Hwang, and Jungho Ryu. Linear and nonlinear dielectric ceramics for high-power energy storage capacitor applications. *Journal of the Korean Ceramic Society*, 56(1):1–23, 2019.
- [66] Zhiyang Wang, Deqing Xue, Yumei Zhou, Nan Wang, Xiangdong Ding, Jun Sun, Turab Lookman, and Dezhen Xue. Enhanced energy-storage density by reversible domain switching in acceptor-doped ferroelectrics. *Physical Review Applied*, 15(3):034061, 2021.
- [67] Bin Peng, Zhenkun Xie, Zhenxing Yue, and Longtu Li. Improvement of the recoverable energy storage density and efficiency by utilizing the linear dielectric response in ferroelectric capacitors. *Applied Physics Letters*, 105(5):052904, 2014.

- [68] Mao Ye, Qiu Sun, Xiangqun Chen, Zhaohua Jiang, and Fuping Wang. Effect of eu doping on the electrical properties and energy storage performance of pbzro₃ antiferroelectric thin films. *Journal of the American Ceramic Society*, 94(10):3234–3236, 2011.
- [69] Venkata Sreenivas Puli, Patrick Li, Shiva Adireddy, and Douglas B Chrisey. Crystal structure, dielectric, ferroelectric and energy storage properties of la-doped batio₃ semiconducting ceramics. *Journal of Advanced Dielectrics*, 5(03):1550027, 2015.
- [70] YY Guo, MH Qin, T Wei, KF Wang, and J-M Liu. Kinetics controlled aging effect of ferroelectricity in al-doped and ga-doped batio₃. *Applied Physics Letters*, 97(11):112906, 2010.
- [71] Mohamad M Ahmad, Koji Yamada, Paul Meuffels, and Rainer Waser. Aging-induced dielectric relaxation in barium titanate ceramics. *Applied physics letters*, 90(11):112902, 2007.
- [72] Zechao LI, Shenglan HAO, Eva HERIPRE, and Pierre-Eymeric JANOLIN. Improvement of energy storage of ferroelectric by defect dipoles configuration. unpublished, 2021.
- [73] Methee Promsawat, Marco Deluca, Sirirat Kamposiri, Boonruang Marungsri, and Soodkhet Pojprapai. Electrical fatigue behavior of lead zirconate titanate ceramic under elevated temperatures. *Journal of the European Ceramic Society*, 37(5):2047–2055, 2017.
- [74] Yingying Zhao, Jiping Wang, Lixue Zhang, Chenchen Wang, and Shujuan Liu. Aging rate of cerium doped ba (ti_{0.99}mn_{0.01}) o₃. *Ceramics International*, 43:S70–S74, 2017.
- [75] RC Bradt and GS Ansell. Aging in tetragonal ferroelectric barium titanate. *Journal of the American Ceramic Society*, 52(4):192–198, 1969.
- [76] KnW Plessner. Ageing of the dielectric properties of barium titanate ceramics. *Proceedings of the Physical Society. Section B*, 69(12):1261, 1956.
- [77] AF Devonshire. Theory of ferroelectrics. *Advances in physics*, 3(10):85–130, 1954.
- [78] WL Warren, D Dimos, GE Pike, K Vanheusden, and R Ramesh. Alignment of defect dipoles in polycrystalline ferroelectrics. *Applied physics letters*, 67(12):1689–1691, 1995.
- [79] WL Warren, GE Pike, K Vanheusden, D Dimos, BA Tuttle, and J Robertson. Defect-dipole alignment and tetragonal strain in ferroelectrics. *Journal of applied physics*, 79(12):9250–9257, 1996.
- [80] William L Warren, Karel Vanheusden, Duane Dimos, Gordon E Pike, and Bruce A Tuttle. Oxygen vacancy motion in perovskite oxides. *Journal of the American Ceramic Society*, 79(2):536–538, 1996.
- [81] JF Scott and Matthew Dawber. Oxygen-vacancy ordering as a fatigue mechanism in perovskite ferroelectrics. *Applied Physics Letters*, 76(25):3801–3803, 2000.
- [82] Maxim I Morozov and Dragan Damjanovic. Hardening-softening transition in fe-doped pb (zr, ti) o₃ ceramics and evolution of the third harmonic of the polarization response. *Journal of Applied Physics*, 104(3):034107, 2008.
- [83] LX Zhang, W Chen, and X Ren. Large recoverable electrostrain in mn-doped (ba, sr) ti o₃ ceramics. *Applied Physics Letters*, 85(23):5658–5660, 2004.
- [84] Julia Glaum, Torsten Granzow, Ljubomira Ana Schmitt, Hans-Joachim Kleebe, and Jürgen Rödel. Temperature and driving field dependence of fatigue processes in pzt bulk ceramics. *Acta materialia*, 59(15):6083–6092, 2011.
- [85] Nina Balke, Doru C Lupascu, Torsten Granzow, and Jürgen Rödel. Fatigue of lead zirconate titanate ceramics. i: Unipolar and dc loading. *Journal of the American Ceramic Society*, 90(4):1081–1087, 2007.
- [86] U Robels and G Arlt. Domain wall clamping in ferroelectrics by orientation of defects. *Journal of Applied Physics*, 73(7):3454–3460, 1993.
- [87] Doru C Lupascu, Yuri A Genenko, and Nina Balke. Aging in ferroelectrics. *Journal of the American Ceramic Society*, 89(1):224–229, 2006.
- [88] Xiaobing Ren. Large electric-field-induced strain in ferroelectric crystals by point-defect-mediated reversible domain switching. *Nature materials*, 3(2):91–94, 2004.
- [89] EI Bondarenko, V Yu Topolov, and AV Turik. The role of 90 domain wall displacements in forming physical properties of perovskite ferroelectric ceramics. *Ferroelectrics Letters Section*, 13(1):13–19, 1991.
- [90] Dragan Damjanovic and Marlyse Demartin. Contribution of the irreversible displacement of domain walls to the piezoelectric effect in barium titanate and lead zirconate titanate ceramics. *Journal of Physics: Condensed Matter*, 9(23):4943, 1997.
- [91] Fei Li, Li Jin, Zhuo Xu, and Shujun Zhang. Electrostrictive effect in ferroelectrics: An alternative approach to improve piezoelectricity. *Applied Physics Reviews*, 1(1):011103, 2014.
- [92] Takaaki Tsurumi, Yutaka Kumano, Naoki Ohashi, Tadashi Takenaka, and Osamu Fukunaga. 90° domain reorientation and electric-field-induced strain of tetragonal lead zirconate titanate ceramics. *Japanese journal of applied physics*, 36(9S):5970, 1997.
- [93] Ting Zheng, Jiagang Wu, Dingquan Xiao, and Jianguo Zhu. Recent development in lead-free perovskite piezoelectric bulk materials. *Progress in materials science*, 98:552–624, 2018.
- [94] Bastola Narayan, Jaskaran Singh Malhotra, Rishikesh Pandey, Krishna Yaddanapudi, Pavan Nukala, Brahim Dkhil, Anatoliy Senyshyn, and Rajeev Ranjan. Electrostrain in excess of 1% in polycrystalline piezoelectrics. *Nature materials*, 17(5):427–431, 2018.
- [95] Hans Jaffe. Piezoelectric ceramics. *Journal of the American Ceramic Society*, 41(11):494–498, 1958.
- [96] Thomas R Shrout and Shujun J Zhang. Lead-free piezoelectric ceramics: Alternatives for pzt? *Journal of Electroceramics*, 19(1):113–126, 2007.
- [97] Seung-Eek Park and Thomas R Shrout. Ultrahigh strain and piezoelectric behavior in relaxor based ferroelectric single crystals. *Journal of applied physics*, 82(4):1804–1811, 1997.